Interaction of cracks with dislocations in couple-stress elasticity. Part II: Shear modes

K.P. Baxevanakis [1*], P.A. Gourgiotis [2], H.G. Georgiadis [1]**

[1]*Mechanics Division, National Technical University of Athens, Zographou, GR-15773, Greece*

[2]*School of Engineering & Computing Sciences, Durham University, South Road, Durham, DH1 3LE, UK*

Abstract: In the second part of this study, the interaction of a finite-length crack with a glide and a screw dislocation is examined within the framework of couple-stress elasticity. The loading from the two defects on the crack results to plane and antiplane shear modes of fracture, respectively. Both problems are attacked using the distributed dislocation technique and the cracks are modeled using distributions of discrete glide or screw dislocations. The antiplane strain case is governed by a single hyper-singular integral equation with a cubic singularity, whereas the plane strain case by a singular integral equation. In both cases, the integral equations are numerically solved using appropriate collocation techniques. The results obtained herein show that a crack under antiplane conditions closes in a smoother way as compared to the classical elasticity result. Further, the evaluation of the energy release rate in the crack tips reveals an 'alternating' behavior between strengthening and weakening effects in the plane strain case, depending on the defect's distance from the crack tip and the magnitude of the characteristic material length. On the other hand, the energy release rate in the antiplane mode shows a strengthening effect when couple-stresses are considered.

Keywords: Screw Dislocation; Glide Dislocation; Microstructure; Hyper-singular Integral Equations; couple-stress theory.

[*] Current affiliation: Theoretical & Applied Mechanics Group, Mechanical Engineering & Mechanics Department, Drexel University, 3141 Chestnut Street, Philadelphia, PA 19104, USA.

[**] Corresponding author: H.G. Georgiadis. *E-mail* address: georgiad@central.ntua.gr

1. Introduction

In Part II of this study, the interaction problems of a finite-length crack with a glide[2] and a screw dislocation are examined in the framework of couple-stress-theory. Both defects lie along the crack plane and are not emitted from the crack-tip. The glide dislocation results in an in-plane shear mode, while the screw dislocation produces a purely antiplane deformation. The problems are tackled employing the distributed dislocation technique (DDT). The DDT has its origins in the pioneering works of Bilby et al. (1963) and Bilby and Eshelby (1968). Ever since, it has been utilized to analyze various crack problems in classical elasticity and more recently has been extended in the context of couple-stress elasticity (Gourgiotis and Georgiadis, 2007, 2008). The main advantage of the technique is that it provides detailed full-field solutions at the expense of relatively little analytical demands compared e.g. to the technique of dual integral equations while requiring a relatively small computational cost compared to the Finite Element or Boundary Element methods. A thorough review on this technique and its applications is given by Hills et al. (1996).

The two boundary value problems are presented in parallel in each Section of this article. Contrary to the interaction problem between a finite-length crack and a climb dislocation presented in Part I, the corrective solution for the interaction with a glide dislocation is achieved by a continuous distribution of glide dislocations only. Therefore, the plane shear mode problem is mathematically less involved than the opening mode problem. In classical elasticity the two problems are described by the same singular integral equation. On the other hand, the corrective stresses in the antiplane problem are generated by a continuous distributions of screw dislocations. The stress field for a discrete glide dislocation is obtained using Mindlin's stress functions while those of a discrete screw dislocation using the Fourier integral transform. Moreover, the plane-strain problem is described by a singular integral equation, whereas the antiplane problem by a *hyper-singular* integral equation with a cubic singularity. The integral equations are solved numerically using appropriate collocation techniques. Similar to Part I, the energy release rate (J-integral) in both crack tips is evaluated. In the plane problem an interesting 'alternating' behavior between strengthening and weakening is revealed, depending on the distance of the discrete glide dislocation from the crack tip and the magnitude of the characteristic material length. Finally, in the antiplane

[2] The jargon term 'glide' refers to an edge dislocation with its Burgers vector *parallel* to the cut made to create the defect (Hills et al. 1996).

problem a strengthening effect is observed regardless of the distance of the screw dislocation to the crack tip.

2. Basic equations of couple-stress elasticity in plane and antiplane strain

The couple-stress elasticity is the simplest theory of elasticity in which couple-stresses arise. The basic assumptions in this theory are: (i) every material particle has three degrees of freedom (just as in classical theory), (ii) the Euler-Cauchy Stress Principle is augmented with a non-vanishing couple-stress vector, (iii) the strain energy density depends not only upon the strain tensor (as in classical elasticity) but also upon the gradient of rotation vector (curvature tensor). The basic concepts of the linear three-dimensional couple-stress elasticity can be found in the fundamental papers of Toupin (1962), Mindlin and Tiersten (1962), and Koiter (1964).

2.1 Plane strain

In this Section, we recall briefly certain pertinent elements of the plane strain couple-stress theory that are essential to our analysis. A more detailed description of the plane strain theory can be found in Section 2 in Part I of this study.

In the plane-strain case, the equations of force and moment equilibrium in the absence of body forces and body couples reduce to

$$\frac{\partial \sigma_{xx}}{\partial x}+\frac{\partial \sigma_{yx}}{\partial y}=0\,,\quad \frac{\partial \sigma_{xy}}{\partial x}+\frac{\partial \sigma_{yy}}{\partial y}=0\,,\quad \sigma_{xy}-\sigma_{yx}+\frac{\partial m_{xz}}{\partial x}+\frac{\partial m_{yz}}{\partial y}=0\ . \tag{1}$$

Accordingly, the compatibility equations in terms of the stress and the couple stress components assume the following form (Muki and Sternberg, 1965)

$$\frac{\partial^2 \sigma_{xx}}{\partial y^2}-\frac{\partial^2}{\partial x\partial y}\left(\sigma_{xy}+\sigma_{yx}\right)+\frac{\partial^2 \sigma_{yy}}{\partial x^2}=\nu\nabla^2\left(\sigma_{xx}+\sigma_{yy}\right)\ , \tag{2}$$

$$\frac{\partial m_{xz}}{\partial y}=\frac{\partial m_{yz}}{\partial x}\,, \tag{3}$$

$$m_{xz}=-2\ell^2\frac{\partial}{\partial y}\left[\sigma_{xx}-\nu\left(\sigma_{xx}+\sigma_{yy}\right)\right]+\ell^2\frac{\partial}{\partial x}\left(\sigma_{xy}+\sigma_{yx}\right), \tag{4}$$

$$m_{yz} = 2\ell^2 \frac{\partial}{\partial x}\left[\sigma_{yy} - \nu\left(\sigma_{xx} + \sigma_{yy}\right)\right] - \ell^2 \frac{\partial}{\partial y}\left(\sigma_{xy} + \sigma_{yx}\right). \tag{5}$$

Notice that only three of the four equations of compatibility are independent. Indeed, Eqs (3)-(5) imply (2), while Eqs. (2), (4) and (5) yield Eq. (3).

The complete solution of Eqs. (1) admits the following representation in terms of the Mindlin's stress functions (Mindlin, 1963)

$$\begin{aligned} \sigma_{xx} &= \frac{\partial^2 \Phi}{\partial y^2} - \frac{\partial^2 \Psi}{\partial x \partial y}, \qquad \sigma_{yy} = \frac{\partial^2 \Phi}{\partial x^2} + \frac{\partial^2 \Psi}{\partial x \partial y}, \\ \sigma_{xy} &= -\frac{\partial^2 \Phi}{\partial x \partial y} - \frac{\partial^2 \Psi}{\partial y^2}, \quad \sigma_{yx} = -\frac{\partial^2 \Phi}{\partial x \partial y} + \frac{\partial^2 \Psi}{\partial x^2}, \end{aligned} \tag{6}$$

and

$$m_{xz} = \frac{\partial \Psi}{\partial x}, \quad m_{yz} = \frac{\partial \Psi}{\partial y}, \tag{7}$$

where $\Phi \equiv \Phi(x, y)$ and $\Psi \equiv \Psi(x, y)$ are two arbitrary but sufficiently smooth functions.

Further, substitution of Eqs (6) and (7) into (4) and (5) results in the following pair of differential equations, for the stress functions

$$\frac{\partial}{\partial x}\left(\Psi - \ell^2 \nabla^2 \Psi\right) = -2(1-\nu)\ell^2 \nabla^2 \left(\frac{\partial \Phi}{\partial y}\right), \tag{8}$$

$$\frac{\partial}{\partial y}\left(\Psi - \ell^2 \nabla^2 \Psi\right) = 2(1-\nu)\ell^2 \nabla^2 \left(\frac{\partial \Phi}{\partial x}\right), \tag{9}$$

which, accordingly, lead to the uncoupled PDEs

$$\nabla^4 \Phi = 0, \quad \nabla^2 \Psi - \ell^2 \nabla^4 \Psi = 0. \tag{10}$$

Note that the above representation reduces to the classical Airy's representation as the quantities ℓ, $\partial_x \Psi$, and $\partial_y \Psi$ tend to zero. In addition, one can obtain the following relations

connecting the displacement gradients in terms of Mindlin's stress functions (Muki and Sternberg, 1965)

$$\frac{\partial u_x}{\partial x}=\frac{1}{2\mu}\left(\frac{\partial^2\Phi}{\partial y^2}-\frac{\partial^2\Psi}{\partial x\partial y}-\nu\nabla^2\Phi\right), \tag{11}$$

$$\frac{\partial u_y}{\partial y}=\frac{1}{2\mu}\left(\frac{\partial^2\Phi}{\partial x^2}+\frac{\partial^2\Psi}{\partial x\partial y}-\nu\nabla^2\Phi\right), \tag{12}$$

$$\frac{\partial u_x}{\partial y}+\frac{\partial u_y}{\partial x}=-\frac{1}{2\mu}\left(2\frac{\partial^2\Phi}{\partial x\partial y}-\frac{\partial^2\Psi}{\partial x^2}+\frac{\partial^2\Psi}{\partial y^2}\right). \tag{13}$$

2.2 Antiplane strain

Next, we consider a body that occupies a domain in the (x, y)-plane under antiplane strain conditions. In this case, the displacement field reduces to

$$u_x=u_y=0\,,\qquad u_z\equiv w\neq 0\,,\qquad w\equiv w(x,y)\,. \tag{14}$$

The non-vanishing components of the strain tensor, the rotation vector, and the curvature tensor are defined as (Lubarda, 2003)

$$\varepsilon_{xz}=\frac{1}{2}\frac{\partial w}{\partial x}\,,\qquad \varepsilon_{yz}=\frac{1}{2}\frac{\partial w}{\partial y}\,,\qquad \omega_x=\frac{1}{2}\frac{\partial w}{\partial y}\,,\qquad \omega_y=-\frac{1}{2}\frac{\partial w}{\partial x}\,, \tag{15}$$

$$\kappa_{xx}=-\kappa_{yy}=\frac{1}{2}\frac{\partial^2 w}{\partial x\partial y}\,,\qquad \kappa_{xy}=-\frac{1}{2}\frac{\partial^2 w}{\partial x^2}\,,\qquad \kappa_{yx}=\frac{1}{2}\frac{\partial^2 w}{\partial y^2}\,. \tag{16}$$

Assuming further a linear and isotropic material response the strain energy density takes the following form

$$W=2\mu\left(\varepsilon_{xz}^2+\varepsilon_{yz}^2\right)+2\left(\eta+\eta'\right)\left(\kappa_{xx}^2+\kappa_{yy}^2\right)+2\eta\left(\kappa_{xy}^2+\kappa_{yx}^2\right)+4\eta'\kappa_{xy}\kappa_{yx}\,, \tag{17}$$

where μ have the same meaning as the shear modulus in the classical theory, and (η,η') are the couple-stress moduli with dimensions of $[\,force]$. Note that for the strain energy density to be positive definite, the elastic moduli must satisfy the following inequalities

$$\mu > 0\ , \qquad \eta > 0\ , \qquad -1 < \eta'/\eta < 1\ . \tag{18}$$

The stress and couple-stress components are written in terms of the displacement field as

$$\sigma_{xz} = \mu \frac{\partial}{\partial x}\left(w - \ell^2 \nabla^2 w\right), \qquad \sigma_{zx} = \mu \frac{\partial}{\partial x}\left(w + \ell^2 \nabla^2 w\right)\ , \tag{19}$$

$$\sigma_{yz} = \mu \frac{\partial}{\partial y}\left(w - \ell^2 \nabla^2 w\right), \qquad \sigma_{zy} = \mu \frac{\partial}{\partial y}\left(w + \ell^2 \nabla^2 w\right)\ . \tag{20}$$

$$m_{xx} = 4\left(\eta + \eta'\right)\kappa_{xx} = 2\left(\eta + \eta'\right)\frac{\partial^2 w}{\partial x \partial y}\ , \tag{21}$$

$$m_{yy} = 4\left(\eta + \eta'\right)\kappa_{yy} = -2\left(\eta + \eta'\right)\frac{\partial^2 w}{\partial x \partial y} = -m_{xx}\ , \tag{22}$$

$$m_{xy} = 4\eta\kappa_{xy} + 4\eta'\kappa_{yx} = -2\eta\frac{\partial^2 w}{\partial x^2} + 2\eta'\frac{\partial^2 w}{\partial y^2}\ , \tag{23}$$

$$m_{yx} = 4\eta\kappa_{yx} + 4\eta'\kappa_{xy} = 2\eta\frac{\partial^2 w}{\partial y^2} - 2\eta'\frac{\partial^2 w}{\partial x^2}\ . \tag{24}$$

with $\ell = \eta/\mu$ being the characteristic material length of couple-stress isotropic elasticity.

For future purposes, we also cite the pertinent tractions that can be prescribed on a surface defined by the unit normal $\mathbf{n} = (0, \pm 1)$ (Mindlin and Tiersten, 1962)

$$P_z^{(n)} \equiv t_{yz} = \sigma_{yz} + \frac{1}{2}\partial_x m_{yy}\ , \qquad R_x^{(n)} = m_{yx}\ . \tag{25}$$

where t_{yz} denotes the total shear stress.

Finally, combining the Eqs (14)-(24), a scalar equilibrium equation is obtained in terms of the out-of-plane displacement

$$\nabla^2 w - \ell^2 \nabla^4 w = 0\ . \tag{26}$$

It is worth noting that Eq. (26) describes also the bending of Kirchhoff plate with uniform prestress.

3. Formulation of the crack problems

3.1 Interaction of a finite-length crack with a glide dislocation

Consider a straight crack of finite length $2a$ in an infinite elastic couple-stress medium and a discrete glide dislocation with Burgers vector $\mathbf{b}=(b_x, 0, 0)$ lying at a distance d from the center of the crack (Fig. 1). Plane strain conditions prevail and the dislocation field is the only loading applied to the body. The crack faces are described by the outward normal unit vector $\mathbf{n}=(0, \pm 1)$ and remain traction free. The following boundary conditions along the crack faces hold

$$\sigma_{yy}(x, 0)=0, \quad \sigma_{yx}(x, 0)=0, \quad m_{yz}(x, 0)=0, \qquad \text{for} \quad |x|<a \ . \tag{27}$$

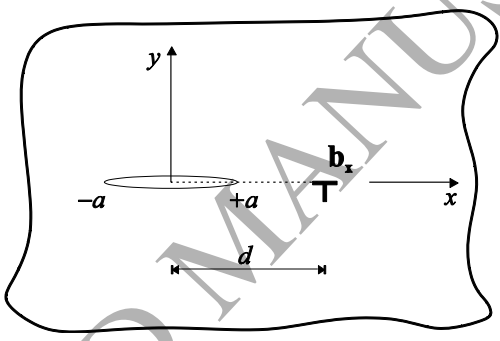

Fig. 1: Interaction of a finite length crack with a discrete glide dislocation.

Further, the regularity conditions at infinity are

$$\sigma_{pq}^{\infty} \to 0, \quad m_{qz}^{\infty} \to 0, \quad \text{as} \quad r \to \infty \ , \tag{28}$$

where $(p,q)=(x,y)$ and $r=(x^2+y^2)^{1/2}$ is the distance from the origin. Equations (28) suggest that there is no other remote loading to the body except the one induced by the discrete dislocation.

Moreover, as it is shown in Gourgiotis and Georgiadis (2007), a discrete glide dislocation lying at the crack plane ($y=0$) in an *infinite* isotropic couple-stress medium

induces only shear stresses $\sigma_{yx}^{(b_x)}(x,0)$ along the crack faces, so that $\sigma_{yy}^{(b_x)}(x,0)=0$ and $m_{yz}^{(b_x)}(x,0)=0$ (c.f. (42), Section 4.1).

In order to obtain a solution for this problem, two auxiliary problems are considered. First, we consider an *un-cracked* body subjected to the loading $\sigma_{yx}^{(b_x)}(x-d,0)$ of the discrete glide dislocation placed along the crack line ($y=0$) and at a distance d from the crack center (origin of the axes). Accordingly, a second auxiliary problem is considered in order to generate the corrective solution. A geometrically identical body to the cracked case is studied, however, without the loading of the discrete glide dislocation. The only loading in this geometry is applied along the crack faces and consists of equal and opposite tractions to those generated in the first auxiliary problem. Thus, the boundary conditions of this problem are

$$\sigma_{yy}(x,0)=0, \quad \sigma_{yx}(x,0)=-\sigma_{yx}^{(b_x)}(x-d,0), \quad m_{yz}(x,0)=0 \quad \text{for } |x|<a, \qquad (29)$$

augmented with the regularity conditions (28). It is worth noting that contrary to the problem of the interaction of a finite-length crack with a discrete climb dislocation examined in Part I, in the present case, in order to satisfy the boundary conditions (29), it is sufficient to distribute only glide dislocations along the crack faces, since the latter defect does not induce any normal stresses or couple-stresses along the crack plane ($y=0$) (c.f. Eqs (42)). Therefore, the first and third of Eqs (29) are automatically satisfied. In the framework of classical elasticity, the problem is described by the first and second of (29), which are also satisfied by a distribution of discrete glide dislocations along the crack faces.

The shear stress $\sigma_{yx}^{(b_x)}(x-d,0)$ generated by a discrete glide dislocation at a distance d from the origin is given in Eq. (41) of Section 4.1. This stress will serve as the influence function for the plane shear mode crack problem under consideration.

3.2 Interaction of a finite-length crack with a screw dislocation

The interaction problem between a finite-length crack and a screw dislocation is considered next in the framework of couple-stress theory. The geometrical configuration is the same as before: the crack length is $2a$ and the distance of the defect from the center of the crack is equal to d (Fig. 2). Antiplane strain conditions prevail and the only loading applied to the

body is that of a screw dislocation with Burgers vector $\mathbf{b}=(0,\,0,\,b_z)$. Note that the problem of an antiplane crack under remote mode III loading in couple-stress elasticity was investigated by Gourgiotis and Georgiadis (2007) and Radi (2008), while the steady state dynamic case was examined by Mishuris et al. (2012).

In view of Eqs (25), the crack problem is described by the following boundary conditions

$$t_{yz}(x,0)=\sigma_{yz}(x,\,0)+\frac{1}{2}\partial_x m_{yy}(x,\,0)=0\ ,\quad m_{yx}(x,\,0)=0\qquad \text{for}\qquad |x|<a\ , \tag{30}$$

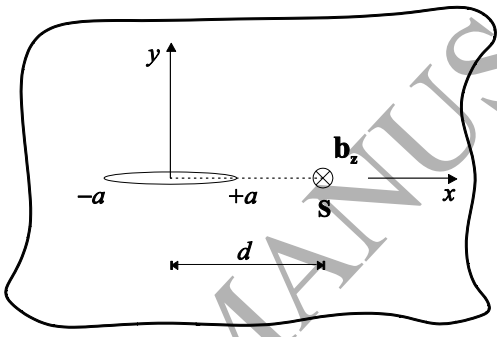

Fig. 2: Interaction of a finite length antiplane crack with a discrete screw dislocation.

along with the regularity conditions at infinity

$$\sigma_{pz}^{\infty}\to 0,\quad m_{pq}^{\infty}\to 0,\qquad \text{as}\qquad r\to\infty\ , \tag{31}$$

where $(p,q)=(x,y)$. Equations (31) suggest that there is no other remote loading to the body except the one induced by the screw discrete dislocation. As it was shown by Gourgiotis and Georgiadis (2007), a discrete screw dislocation in couple-stress elasticity generates only shear stresses $t_{yz}^{(b_z)}(x,0)$ along the crack plane ($-\infty<x<\infty$, $y=0$), so that $m_{yx}^{(b_z)}(x,\,0)=0$ (see also Section 4.2).

As in the plane strain case, the original problem is decomposed into two auxiliary problems: (i) the *un-cracked* body subjected to the shear loading $t_{yz}^{(b_z)}(x-d,0)$ due to the discrete screw dislocation placed at a distance d from the crack center (origin of the axes). (ii) the corrective solution where the cracked body is loaded along the crack faces with equal and opposite tractions to those generated in the first auxiliary problem. Thus, the boundary conditions of the corrective solution are

$$t_{yz}(x,0) = -t_{yz}^{(b_z)}(x-d,0) = -\sigma_{yz}^{(b_z)}(x-d,\,0) - \frac{1}{2}\partial_x m_{yy}^{(b_z)}(x-d,\,0),$$
$$m_{yx}(x,\,0) = 0 \quad \text{for} \quad |x| < a \ , \tag{32}$$

augmented with the regularity conditions (31).

The total shear stress $t_{yz}^{(b_z)}(x-d,0)$ generated by a discrete screw dislocation in isotropic infinite couple-stress medium is given in Eq. (49) in Section 4.2. This stress will serve as the influence function for the antiplane shear mode crack problem under consideration.

4. Influence functions

The stress fields of a glide and a screw dislocation in an infinite couple-stress medium are obtained in this Section. These fields are derived either by employing a stress functions approach or by using Fourier transforms.

4.1 A glide dislocation in couple-stress elasticity

A discrete glide dislocation with Burgers vector $\mathbf{b} = (b_x,\,0,\,0)$ is imposed at the origin of the $(x,\,y)$-plane. In the framework of couple-stress elasticity, the appropriate Mindlin's stress functions for this problem have been presented by Cohen (1966), Knésl and Semela (1972), and Nowacki (1974)

$$\Phi = -\frac{\mu b_x r}{4\pi(1-\nu)}(2\ln r + 1)\sin\theta \ , \tag{33}$$

$$\Psi = \frac{2\mu b_x \ell}{\pi}\left[K_1\left(\frac{r}{\ell}\right) - \frac{\ell}{r}\right]\cos\theta \ , \tag{34}$$

where $r = \left(x^2 + y^2\right)^{1/2}$, $\theta = \tan^{-1}\left(y/x\right)$ and $K_i\left(r/\ell\right)$ is the i^{th} order modified Bessel function of the second kind. Substituting Eqs (33) and (34) into (19)-(24) , we derive the stress fields for a glide dislocation in an infinite isotropic medium as

$$\begin{aligned}\sigma_{xx}^{(b_x)} = &-\frac{\mu b_x}{4\pi(1-\nu)r}(3\sin\theta + \sin 3\theta) + \frac{2\mu b_x}{\pi r}\left[\frac{2\ell^2}{r^2} - K_2\left(\frac{r}{\ell}\right)\right]\sin 3\theta \\ &-\frac{\mu b_x}{4\pi\ell^2} r\left[K_2\left(\frac{r}{\ell}\right) - K_0\left(\frac{r}{\ell}\right)\right](\sin\theta + \sin 3\theta) \ ,\end{aligned} \tag{35}$$

$$\begin{aligned}\sigma_{yy}^{(b_x)} = &\frac{\mu b_x}{4\pi(1-\nu)r}(\sin 3\theta - \sin\theta) - \frac{2\mu b_x}{\pi r}\left[\frac{2\ell^2}{r^2} - K_2\left(\frac{r}{\ell}\right)\right]\sin 3\theta \\ &+\frac{\mu b_x}{4\pi\ell^2} r\left[K_2\left(\frac{r}{\ell}\right) - K_0\left(\frac{r}{\ell}\right)\right](\sin\theta + \sin 3\theta) \ ,\end{aligned} \tag{36}$$

$$\begin{aligned}\sigma_{xy}^{(b_x)} = &\frac{\mu b_x}{4\pi(1-\nu)r}(\cos\theta + \cos 3\theta) - \frac{2\mu b_x}{\pi r}\left[\frac{2\ell^2}{r^2} - K_2\left(\frac{r}{\ell}\right)\right]\cos 3\theta \\ &-\frac{\mu b_x}{4\pi\ell^2} r\left[K_2\left(\frac{r}{\ell}\right) - K_0\left(\frac{r}{\ell}\right)\right](\cos\theta - \cos 3\theta) \ ,\end{aligned} \tag{37}$$

$$\begin{aligned}\sigma_{yx}^{(b_x)} = &\frac{\mu b_x}{4\pi(1-\nu)r}(\cos\theta + \cos 3\theta) - \frac{2\mu b_x}{\pi r}\left[\frac{2\ell^2}{r^2} - K_2\left(\frac{r}{\ell}\right)\right]\cos 3\theta \\ &+\frac{\mu b_x}{4\pi\ell^2} r\left[K_2\left(\frac{r}{\ell}\right) - K_0\left(\frac{r}{\ell}\right)\right](3\cos\theta + \cos 3\theta) \ ,\end{aligned} \tag{38}$$

$$m_{xz}^{(b_x)} = \frac{\mu b_x}{\pi}\left[\frac{2\ell^2}{r^2} - K_2\left(\frac{r}{\ell}\right)\right]\cos 2\theta - \frac{\mu b_x}{\pi} K_0\left(\frac{r}{\ell}\right) \ , \tag{39}$$

$$m_{yz}^{(b_x)} = \frac{\mu b_x}{\pi}\left[\frac{2\ell^2}{r^2} - K_2\left(\frac{r}{\ell}\right)\right]\sin 2\theta \ . \tag{40}$$

Employing the asymptotic relations for the modified Bessel functions (see Part I, Eq. (21)), we observe that as $r \to 0$, the stresses σ_{pq} retain the Cauchy type singularity that arises in classical elasticity. On the other hand, the couple-stress m_{xz} exhibits a logarithmic singularity

while the couple-stress m_{yz} is bounded as $r \to 0$. The stress field reduces to the corresponding solution of classical elasticity as $\ell \to 0$.

Finally, from Eqs (36), (38) and (40), we obtain the following tractions for $y = 0$ at a surface defined by $\mathbf{n} = (0,1)$

$$\sigma_{yx}^{(b_x)}(x,0) = \frac{\mu b_x}{2\pi(1-\nu)x} - \frac{2\mu b_x}{\pi x}\left[\frac{2\ell^2}{x^2} - K_2\left(\frac{|x|}{\ell}\right)\right] + \frac{\mu b_x}{\pi \ell^2} x\left[K_2\left(\frac{|x|}{\ell}\right) - K_0\left(\frac{|x|}{\ell}\right)\right], \tag{41}$$

$$\sigma_{yy}^{(b_x)}(x,0) = 0, \quad m_{yz}^{(b_x)}(x,0) = 0. \tag{42}$$

Eq. (41) is the influence function for the interaction problem of a finite-length crack and a glide dislocation in couple-stress theory presented in Section 3.1.

4.2 A screw dislocation in couple-stress elasticity

The stress field generated by a screw dislocation with Burgers vector $\mathbf{b} = (0,0,b_z)$ in an infinite isotropic couple-stress medium has been derived previously by Gourgiotis and Georgiadis (2007) using the Fourier integral transform method. The out-of-plane displacement in that case becomes

$$w = \frac{b_z}{2\pi}\theta - \frac{b_z}{4\pi}(1+\beta)\left[\frac{2\ell^2}{r^2} - K_2\left(\frac{r}{\ell}\right)\right]\sin 2\theta \ . \tag{43}$$

with $\beta = \eta'/\eta$. It should be noted that only the first term in Eq. (43) contributes to the displacement discontinuity while the quantity within the bracket is continuous and bounded as $r \to 0$. Therefore, the displacement w remains bounded as we move towards the dislocation core similarly to the classical elasticity solution.

Accordingly, the stress field for a discrete screw dislocation in couple-stress elasticity is obtained by substituting Eq. (43) to the constitutive relations (19)-(24)

$$\sigma_{xz}^{(b_z)} = -\frac{\mu b_z}{2\pi r}\sin\theta + \frac{\mu b_z \ell^2 (1+\beta)}{\pi r^3}\sin 3\theta \ , \tag{44}$$

$$\sigma_{yz}^{(b_z)} = \frac{\mu b_z}{2\pi r}\cos\theta - \frac{\mu b_z \ell^2 (1+\beta)}{\pi r^3}\cos 3\theta \, , \tag{45}$$

$$\begin{aligned} m_{yy}^{(b_z)} = -m_{xx}^{(b_z)} = {} & \frac{\mu b_z \ell^2 (1+\beta)}{\pi r^2}\cos 2\theta - \frac{3\mu b_z \ell^2 (1+\beta)^2}{\pi r^2}\left[\frac{2\ell^2}{r^2} - K_2\left(\frac{r}{\ell}\right)\right]\cos 4\theta \\ & - \frac{\mu b_z (1+\beta)^2}{8\pi}\left[K_0\left(\frac{r}{\ell}\right) + \left(3K_0\left(\frac{r}{\ell}\right) - 4K_2\left(\frac{r}{\ell}\right)\right)\cos 4\theta\right] \end{aligned} \, , \tag{46}$$

$$\begin{aligned} m_{yx}^{(b_z)} = {} & \frac{\mu b_z (1+\beta)}{2\pi}\left[\frac{2\ell^2}{r^2} - K_2\left(\frac{r}{\ell}\right)\right]\left[\frac{6(1+\beta)\ell^2}{r^2}\sin 4\theta - \sin 2\theta\right] \\ & - \frac{\mu b_z (1+\beta)^2}{8\pi}\left[2K_2\left(\frac{r}{\ell}\right)\sin 2\theta - \left(3K_0\left(\frac{r}{\ell}\right) - 4K_2\left(\frac{r}{\ell}\right)\right)\sin 4\theta\right] \end{aligned} \, , \tag{47}$$

$$\begin{aligned} m_{xy}^{(b_z)} = {} & \frac{\mu b_z (1+\beta)^2}{\pi}\left[\frac{3\ell^2}{r^2}\left(\frac{2\ell^2}{r^2} - K_2\left(\frac{r}{\ell}\right)\right) + \frac{1}{8}\left(3K_0\left(\frac{r}{\ell}\right) - 4K_2\left(\frac{r}{\ell}\right)\right)\right]\sin 4\theta \\ & - \frac{\mu b_z (1+\beta)}{2\pi}\left[\frac{2\ell^2}{r^2} + \frac{(1-\beta)}{2}K_2\left(\frac{r}{\ell}\right)\right]\sin 2\theta \end{aligned} \, . \tag{48}$$

Regarding the characteristics of the above stress field, the following points are of notice: (i) Based on the asymptotic behavior or the modified Bessel functions (see Part I, Eq. (21)), we conclude that the shear stresses exhibit an r^{-3} singularity, whereas the couple-stresses behave as r^{-2} at the dislocation core. (ii) As $\beta \to -1$ (i.e. $\eta = -\eta'$), the above stress field reduces to the corresponding classical elasticity field.

Finally, in view of Eqs (45)-(47), it is noted that on the crack plane ($y = 0$) we have $m_{yx}^{(b_z)}(x,0) = 0$, while the total shear stress becomes

$$t_{yz}^{(b_z)}(x,0)=\sigma_{yz}^{(b_z)}(x,0)+\frac{1}{2}\partial_x m_{yy}^{(b_z)}(x,0)=$$

$$=\frac{\mu b_z}{2\pi x}-\frac{2\mu b\ell^2(1+\beta)}{\pi x^3}+\frac{6\mu b_z\ell^2(1+\beta)^2}{\pi x^3}\left[\frac{2\ell^2}{x^2}-K_2\left(\frac{|x|}{\ell}\right)\right]. \qquad (49)$$

$$-\frac{\mu b_z(1+\beta)^2}{4\pi x}\left[5K_2\left(\frac{|x|}{\ell}\right)-3K_0\left(\frac{|x|}{\ell}\right)\right]$$

It is remarked that the shear stress t_{yz} exhibits a cubic singularity x^{-3} as $x\to 0$. Equation (49) is the influence function for the interaction problem of a finite-length crack and a screw dislocation in couple-stress theory presented in Section 3.2. For $\beta=-1$ it reduces to the corresponding influence function of classical elasticity (Bilby, 1968).

5. Integral equation approach

5.1 Interaction of a finite-length crack with a glide dislocation

In order to generate the corrective solution stresses (Eq. (29)), discrete glide dislocations need to be distributed along the crack faces. The elastic field generated by the continuous distribution of these defects is derived by integrating the influence function (Eq. (41)) along the crack faces. The first and third of Eq. (29) are automatically satisfied, so that a single integral equation is obtained. Employing asymptotic analysis, we separate the singular from the regular part of the kernel and obtain the following singular integral equation

$$-\sigma_{yx}^{(b_x)}(x-d,0)=\frac{\mu(3-2\nu)}{2\pi(1-\nu)}\int_{-a}^{a}\frac{B_{II}(t)}{x-t}dt+\frac{\mu}{\pi}\int_{-a}^{a}B_{II}(t)R_4(x-t)dt\,,\quad |x|<a\,. \qquad (50)$$

The quantity $B_{II}(t)=db_x(t)/dt=-d\left(\Delta u_x(t)\right)/dt$ is the glide dislocation density at a point t $(|t|<a)$, where $\Delta u_x=u_x(t,0^+)-u_x(t,0^-)$ is the relative tangential displacement between the upper and lower crack faces. The kernel $R_4(x-t)$ is given as

$$R_4(x-t)=-\frac{2}{x-t}\left[\frac{2\ell^2}{(x-t)^2}-K_2\left(\frac{|x-t|}{\ell}\right)-\frac{1}{2}\right]$$

$$-\frac{(x-t)}{\ell^2}\left[\frac{2\ell^2}{(x-t)^2}-K_2\left(\frac{|x-t|}{\ell}\right)+K_0\left(\frac{|x-t|}{\ell}\right)\right], \qquad (51)$$

and it can be readily shown, using the asymptotic properties of the modified Bessel functions, that is regular as $x \to t$.

Further, in order to ensure uniqueness of the values of the tangential displacement for a closed loop around the crack, the following closure condition must hold

$$\int_{-1}^{1} B_{II}\left(\tilde{t}\right) d\tilde{t} = 0 \ . \tag{52}$$

In the special case that the discrete dislocation lies at the crack-tip, the LHS of Eq. (50) tends to zero and the contribution of the defect is described by letting Eq. (52) be equal to the Burgers vector b_x of the discrete glide dislocation (Markenscoff, 1993).

Regarding now the asymptotic behavior of the tangential displacement u_x, Huang et al. (1997) showed that in the framework of couple-stress theory it behaves as $\sim R^{1/2}$ near the crack tips, where R is the radial distance from the crack tip. Thus, the glide dislocation density behaves as $\sim R^{-1/2}$ and can be written as

$$B_{II}\left(\tilde{t}\right) = \sum_{n=0}^{\infty} b_n T_n\left(\tilde{t}\right)\left(1-\tilde{t}^{\,2}\right)^{-1/2} \ , \quad \left|\tilde{t}\right| < 1, \tag{53}$$

where $T_n\left(\tilde{t}\right)$ are the Chebyshev polynomials of the first kind, b_n are unknown parameters and $\tilde{t} = t/a$.

The singular (Cauchy) integral in Eq. (50) is calculated in closed form using Eq. (A1) in Appendix A. Also, due to the complementary condition (52), the constant b_0 turns out to be zero. Based on the above considerations and after appropriate normalization over the interval $\left[-1, 1\right]$, the integral equation (50) is written in the following discretized form

$$-\sigma_{yx}^{(b_x)}\left(a\tilde{x} - a\tilde{d},\, 0\right) = -\frac{\mu\left(3-2\nu\right)}{2\left(1-\nu\right)} \sum_{n=1}^{\infty} b_n U_{n-1}\left(\tilde{x}\right) + \frac{\mu}{\pi} \sum_{n=1}^{\infty} b_n \, Q_n^{(4)}\left(\tilde{x}\right), \qquad \left|\tilde{x}\right| < 1 \ , \tag{54}$$

where $\tilde{x} = x/a$, $\tilde{d} = d/a$ and the function $Q_n^{(4)}\left(\tilde{x}\right)$ is defined as

$$Q_n^{(4)}(\tilde{x}) = \int_{-1}^{1} T_n(\tilde{t})\left(1-\tilde{t}^2\right)^{-1/2} R_4(a\tilde{x}-a\tilde{t})\,d\tilde{t} \ . \tag{55}$$

Note that the regular integral in (55) is evaluated using the standard Gauss-Chebyshev quadrature.

Eq. (54) is solved numerically by truncating the series at $n=N$ and using an appropriate collocation technique, where the collocation points are chosen as the roots of the second kind Chebyshev polynomial $U_N(\tilde{x})$, viz. $\tilde{x}_j = \cos\left(j\pi/(N+1)\right)$ with $j=1,2,...,N$. The convergence of the solution depends on the ratio ℓ/a as shown in Table 1 (Section 7).

5.2 Interaction of a finite-length crack with a screw dislocation

As in the shear mode crack problem, the generation of the corrective solution stresses (Eq. (32)) is achieved by a continuous distribution of screw dislocations. The desired elastic field is produced by integrating the influence function (Eq. (49)) along the crack faces. In this way, a single integral equation that governs the problem is obtained. With the use of asymptotic analysis, we separate the singular from the regular part of the kernel and obtain the following governing equation

$$\begin{aligned} -t_{yz}^{(b_z)}(x-d,\,0) = -c_1\ell^2\ \text{F.P.}\int_{-a}^{a}\frac{B_{III}(t)}{(x-t)^3}\,dt + c_2\int_{-a}^{a}\frac{B_{III}(t)}{x-t}\,dt \\ +c_3\int_{-a}^{a} B_{III}(t)\ R_5(x-t)\,dt, \qquad |x|<a \end{aligned} \ , \tag{56}$$

where the symbol F.P. denotes a Hadamard finite-part integral (see e.g. Kutt, 1975; Monegato, 1994). Equation (56) is a hyper-singular integral equation with cubic and Cauchy type singularities. The screw dislocation density at a point t $(|t|<a)$ is defined as $B_{III}(t) = db_z(t)/dt = -d\left(\Delta w(t)\right)/dt$, where $\Delta w = w(t,\,0^+) - w(t,\,0^-)$ is the relative out-of-plane displacement between the upper and lower crack faces. The constants c_q, with $q=1,\,2,\,3$, are given as

$$c_1 = \frac{\mu(1+\beta)(3-\beta)}{2\pi}\ , \qquad c_2 = \frac{\mu\left(\beta^2+2\beta+9\right)}{16\pi}\ , \qquad c_3 = \frac{\mu(1+\beta)^2}{\pi}\ , \tag{57}$$

and the regular kernel $R_5(x-t)$ as

$$R_5(x-t) = -\frac{\ell^2}{(x-t)^3}\left[6\left(K_2\left(\frac{|x-t|}{\ell}\right)-\frac{2\ell^2}{(x-t)^2}\right)+\frac{1}{2}\right] + \frac{1}{4(x-t)}\left[3K_0\left(\frac{|x-t|}{\ell}\right)-5K_2\left(\frac{|x-t|}{\ell}\right)-\frac{1}{4}\right] . \tag{58}$$

It is interesting to note that for $\beta = -1$, Eq. (56) reduces to the corresponding governing equation in classical elasticity.

In the framework of couple-stress theory, Zhang et al. (1998) employed the asymptotic Williams technique to show that the antiplane displacement w behaves as $\sim R^{3/2}$ near the crack tip region. Therefore, the screw dislocation density behaves as $\sim R^{1/2}$ and can be written as

$$B_{III}(\tilde{t}) = \sum_{n=0}^{\infty} b_n U_n(\tilde{t})\left(1-\tilde{t}^2\right)^{1/2} , \quad |\tilde{t}| < 1 , \tag{59}$$

where $U_n(\tilde{t})$ are the Chebyshev polynomials of the second kind. Also, the following closure condition holds in order to ensure uniqueness of the values of the antiplane displacement for a closed loop around the crack

$$\int_{-1}^{1} B_{III}(\tilde{t})\, d\tilde{t} = 0 . \tag{60}$$

After appropriate normalization over the interval $[-1, 1]$, the integral equation (56) takes the following form for $|\tilde{x}| < 1$

$$-t_{yz}^{(b_z)}\left(a\tilde{x}-a\tilde{d},\,0\right)=-\frac{c_1\ell^2}{a^2}\sum_{n=0}^{\infty}b_n\,\text{F.P.}\int_{-1}^{1}\frac{U_n\left(\tilde{t}\right)\left(1-\tilde{t}^{\,2}\right)^{1/2}}{\left(\tilde{x}-\tilde{t}\right)^3}d\tilde{t}$$
$$+c_2\sum_{n=0}^{\infty}b_n\int_{-1}^{1}\frac{U_n\left(\tilde{t}\right)\left(1-\tilde{t}^{\,2}\right)^{1/2}}{\tilde{x}-\tilde{t}}d\tilde{t}+c_3\sum_{n=0}^{\infty}b_n\,Q_n^{(5)}\left(\tilde{x}\right) \quad , \tag{61}$$

with $\tilde{x}=x/a$, $\tilde{d}=d/a$, and the function $Q_n^{(5)}\left(\tilde{x}\right)$ is defined as

$$Q_n^{(5)}\left(\tilde{x}\right)=\int_{-1}^{1}U_n\left(\tilde{t}\right)\left(1-\tilde{t}^{\,2}\right)^{1/2}R_5\left(a\tilde{x}-a\tilde{t}\right)d\tilde{t}\ . \tag{62}$$

The singular and hyper-singular integrals in Eq. (61) are calculated in closed form using Eqs (A2) and (A3) in Appendix A, whereas the regular integral in Eq. (62) is evaluated using the standard Gauss-Chebyshev quadrature. The closure condition (Eq. (60)) dictates that the constant b_0 is equal to zero. In view of the above, the hyper-singular integral equation (61) is written in the following discretized form

$$-t_{yz}^{(b_z)}\left(a\tilde{x}-a\tilde{d},\,0\right)=\frac{\pi\ell^2c_1}{4a^2\left(1-\tilde{x}^2\right)}\sum_{n=1}^{\infty}b_n\left[\left(n^2+n\right)U_{n+1}\left(\tilde{x}\right)-\left(n^2+3n+2\right)U_{n-1}\left(\tilde{x}\right)\right]$$
$$+c_2\sum_{n=1}^{\infty}b_nT_{n+1}\left(\tilde{x}\right)+c_3\sum_{n=1}^{\infty}b_n\,Q_n^{(5)}\left(\tilde{x}\right),\qquad \left|\tilde{x}\right|<1\,, \tag{63}$$

In order to solve Eq. (63), an appropriate collocation technique is employed. In this case, we select as collocation point the roots of the Chebyshev polynomial $T_{N+1}\left(\tilde{x}\right)$, that is $\tilde{x}_k=\cos\left[\left(2k-1\right)\pi/2\left(N+1\right)\right]$ with $k=1,2,...,N+1$. Equation (63) along with the closure condition (60) comprise an algebraic system of $N+2$ equations with $N+1$ unknowns which is solved in the least-squares sense. Solution convergence is achieved for different numbers N depending on the ratio ℓ/a, as shown in Table 2 (Section 7). Finally, after calculating the unknown parameters b_n, we use Eq. (59) to evaluate the screw dislocation density B_{III}. It should be noted that the numerical scheme followed herein for the solution of the hyper-singular integral equation (56) differs from the approach employed by Gourgiotis and Georgiadis (2007).

6. Evaluation of the energy release rate

6.1 Interaction of a finite-length crack with a glide dislocation

In this Section, the energy release rate (*J*-integral) is derived at both crack tips. In particular, taking into account that in the plane shear mode problem the normal stress σ_{yy} and the couple-stress m_{yz} vanish along the crack plane $y=0$, the *J*-integral takes the simple form (c.f. Eqs (38) and (39) in Part I)

$$J=-2\lim_{\varepsilon\to+0}\left\{\int_{\pm a-\varepsilon}^{\pm a+\varepsilon}\sigma_{yx}\left(x,\,0^{+}\right)\frac{\partial u_x\left(x,\,0^{+}\right)}{\partial x}dx\right\}. \tag{64}$$

The dominant singular behavior for the shear stress σ_{yx} is attributed to the Cauchy integral in Eq. (78). The asymptotic behavior of the shear stress near the right $\left(x\to a^{+}\right)$ and left $\left(x\to -a^{-}\right)$ crack-tips is given as $\left(|\tilde{x}|>1\right)$

$$\begin{cases}\sigma_{yx}\left(x\to a^{+},\,0^{+}\right)=\dfrac{\mu\left(3-2\nu\right)}{2\sqrt{2}\left(1-\nu\right)}\displaystyle\sum_{n=1}^{N}b_n\left(\tilde{x}-1\right)^{-1/2}\\ \sigma_{yx}\left(x\to -a^{-},\,0^{+}\right)=-\dfrac{\mu\left(3-2\nu\right)}{2\sqrt{2}\left(1-\nu\right)}\displaystyle\sum_{n=1}^{N}\left(-1\right)^{n}b_n\left|\tilde{x}+1\right|^{-1/2}\end{cases}. \tag{65}$$

Further, employing the definition of the glide dislocation density, the following asymptotic relations are obtained $\left(|\tilde{x}|<1\right)$

$$\begin{cases}\dfrac{\partial u_x\left(x\to a^{-},\,0^{+}\right)}{\partial x}=-\dfrac{1}{2\sqrt{2}}\displaystyle\sum_{n=1}^{N}b_n\left(1-\tilde{x}\right)^{-1/2}\\ \dfrac{\partial u_x\left(x\to -a^{+},\,0^{+}\right)}{\partial x}=-\dfrac{1}{2\sqrt{2}}\displaystyle\sum_{n=1}^{N}\left(-1\right)^{n}b_n\left(1+\tilde{x}\right)^{-1/2}\end{cases}. \tag{66}$$

To evaluate the *J*-integral, we follow a strictly analogous procedure to the one outlined in Part I of this study (see Section 6, Part I). More specifically, a rectangular shaped contour is used that surrounds the (left or right) crack tip and has vanishing height along the *y*-direction. Employing the asymptotic expressions (65) and (66) in conjunction with Fisher's theorem for

products of singular distributions, the *J*-integrals for the right and left crack tips assume finally the forms

$$J_r = \frac{\mu\pi}{2} a \Lambda_3^{(r)} \qquad \text{and} \qquad J_\ell = -\frac{\mu\pi}{2} a \Lambda_3^{(\ell)}, \tag{67}$$

where

$$\Lambda_3^{(r)} = \frac{(3-2\nu)}{4(1-\nu)}\left(\sum_{n=1}^{N} b_n\right)^2, \quad \Lambda_3^{(\ell)} = \frac{(3-2\nu)}{4(1-\nu)}\left(\sum_{n=1}^{N} (-1)^n b_n\right)^2 \tag{68}$$

6.2 Interaction of a finite-length crack with a screw dislocation

The *J*-integral for the antiplane case is evaluated now at the right and left crack tips. In the antiplane case, the couple-stress m_{yx} vanishes for $y = 0$, so that the *J*-integral is written as

$$J = -2 \lim_{\varepsilon \to +0} \left\{ \int_{a-\varepsilon}^{a+\varepsilon} t_{yz}\left(x, 0^+\right) \frac{\partial w\left(x, 0^+\right)}{\partial x} dx \right\}. \tag{69}$$

The dominant singular behavior for the shear stress t_{yz} ahead of the crack tips is attributed to the hyper-singular integral in Eq. (56). For the right crack tip $x \to a^+$, the total shear stress is given as (see Eq. (A6) in Appendix A)

$$\begin{aligned} t_{yz}\left(x \to a^+, 0^+\right) &= -\frac{c_1 \ell^2}{a^2} \lim_{x \to a^+} \int_{-a}^{a} \frac{B_{III}(t)}{(x-t)^3} dt = -\lim_{\tilde{x} \to 1^+} \frac{c_1 \ell^2}{a^2} \sum_{n=1}^{N} b_n \int_{-1}^{1} \frac{U_n(\tilde{t})\left(1-\tilde{t}^2\right)^{1/2}}{(\tilde{x}-\tilde{t})^3} d\tilde{t} \\ &= -\frac{c_1 \ell^2}{a^2} \frac{\pi}{4\sqrt{2}} \sum_{n=1}^{N} (1+n) b_n (\tilde{x}-1)^{-3/2}, \qquad \tilde{x} > 1 \end{aligned} \tag{70}$$

in a similar manner the total shear stress ahead of the left crack-tip becomes

$$t_{yz}\left(x \to -a^-, 0^+\right) = \frac{c_1 \ell^2}{a^2} \frac{\pi}{4\sqrt{2}} \sum_{n=1}^{N} (-1)^n (1+n) b_n |\tilde{x}+1|^{-3/2}, \qquad \tilde{x} < -1. \tag{71}$$

Moreover, for the screw dislocation density $B_{III}(t)$, the following asymptotic relations hold $(|\tilde{x}|<1)$

$$\begin{cases} \dfrac{\partial w\left(x\to a^{-},0^{+}\right)}{\partial x}=-\dfrac{1}{\sqrt{2}}\displaystyle\sum_{n=1}^{N}(n+1)b_n\left(1-\tilde{x}\right)^{1/2} \\ \dfrac{\partial w\left(x\to -a^{+},0^{+}\right)}{\partial x}=-\dfrac{1}{\sqrt{2}}\displaystyle\sum_{n=1}^{N}(-1)^n(n+1)b_n\left(1+\tilde{x}\right)^{1/2} \end{cases}. \tag{72}$$

In view of the above, the *J*-integral at the right crack tip is given by the expression

$$J_r=-2a\lim_{\varepsilon\to 0}\left\{\Lambda_4^{(r)}\int_{-\varepsilon/a}^{\varepsilon/a}\left(x_{+}\right)^{-3/2}\cdot\left(x_{-}\right)^{1/2}d\bar{x}\right\}=\pi a\,\Lambda_4^{(r)}\ , \tag{73}$$

with

$$\Lambda_4^{(r)}=\frac{\pi\ell^2 c_1}{8a^2}\left(\sum_{n=1}^{N}(n+1)b_n\right)^2\ , \tag{74}$$

where we recall that $\bar{x}=\tilde{x}-1$. Note that the distributions of the bisection type $x_{+}^{-3/2}$ and $x_{-}^{1/2}$ in Eq. (73) are defined in Eq. (45) in the Part I of this study. Moreover, for the evaluation of the integral in (73), use of Fisher's theorem has been made where the product of distributions is computed as: $\left(x_{+}\right)^{-3/2}\cdot\left(x_{-}\right)^{1/2}=-2^{-1}\pi\delta(x)$.

In an analogous manner, the *J*-integral at the left crack tip is given as

$$J_\ell=-\pi a\,\Lambda_4^{(\ell)}, \tag{75}$$

where

$$\Lambda_4^{(\ell)}=\frac{(3-2\nu)}{4(1-\nu)}\left(\sum_{n=1}^{N}(-1)^n(n+1)b_n\right)^2\ . \tag{76}$$

The corresponding values for the *J*-integral in classical elasticity may be evaluated in closed form by utilizing a similar contour as the one used earlier in conjunction with the

elastic fields of the problem (Zhang and Li, 1991). Following this procedure, the following forms for the *J*-integral at the right and left crack tips are obtained

$$J_r = \frac{\mu b_z^2 \left[1-\left(\frac{d+a}{d-a}\right)^{1/2}\right]\left[d-a-\left(d^2-a^2\right)^{1/2}\right]}{8\pi a\left(d-a\right)},$$
$$J_\ell = -\frac{\mu b_z^2 \left[1-\left(\frac{d+a}{d-a}\right)^{1/2}\right]\left[d-a-\left(d^2-a^2\right)^{1/2}\right]}{8\pi a\left(d+a\right)}. \quad (77)$$

7. Results and discussion

In this Section, we proceed to the presentation and discussion of the results obtained for the two crack problems.

7.1 Interaction of a finite-length crack with a glide dislocation

In Fig. 3a, the effect of the ratio a/ℓ on the tangential crack-face displacement is displayed for a discrete glide dislocation lying at a distance $d/a = 2.5$ in a couple-stress medium with Poisson's ratio $\nu = 0.3$. It is observed that as the characteristic length ℓ becomes comparable to the crack length, the crack-face displacements become smaller in magnitude compared to the respective ones in classical elasticity. For instance, the maximum displacement for $a/\ell = 5$ appears reduced by 24% compared to the maximum displacement in the classical elasticity solution. This rigidity effect has already been reported in crack problems in the framework of couple-stress elasticity and has been verified also in the opening mode case examined in the Part I of this study (see Fig. 5, Part I). In Fig. 3b, the effect of the dislocation distance to the crack-face displacements is investigated for a material with $a/\ell = 10$ and $\nu = 0.3$. It is shown that the magnitude of the crack face displacements decreases quickly as the distance of the dislocation to the crack tip increases. This due to the fact that the dislocation loading diminishes as $(x-d)^{-1}$ from the dislocation core.

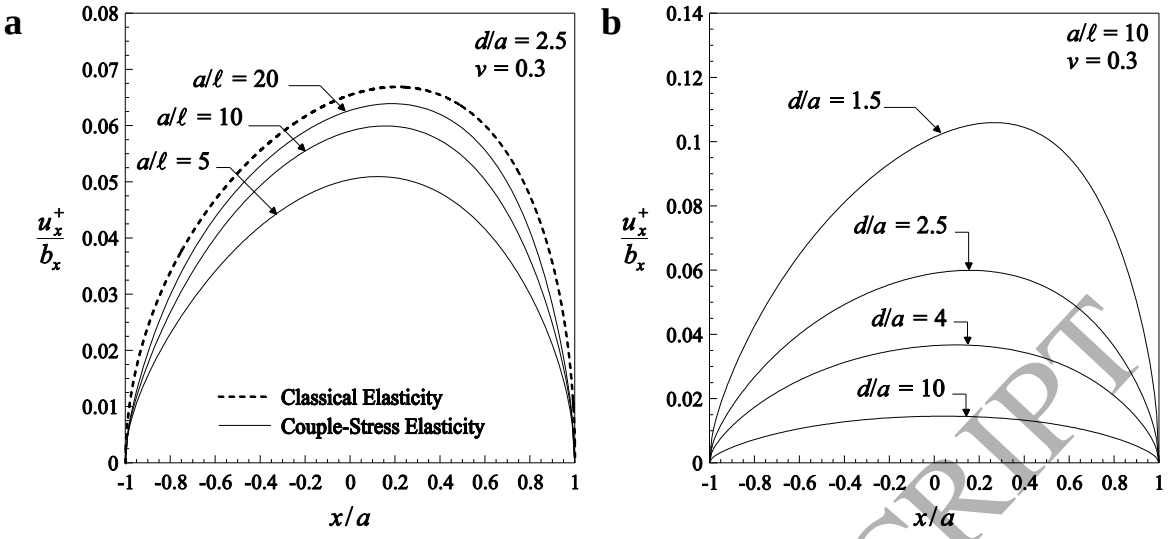

Fig. 3: Normalized upper-half crack tangential displacement profile for **a)** various ratios a/ℓ due to the interaction with a glide dislocation lying at $d/a = 2.5$. **b)** various dislocation positions in a couple-stress material with $a/\ell = 10$. The Poisson's ratio is $\nu = 0.3$ in all cases.

Next, we study the behavior of the shear stress σ_{yx} ahead of the crack tip. Superposing the solutions of the two auxiliary problems, we obtain the following expression

$$\sigma_{yx}\left(|x|>a,\,0\right)=\sigma_{yx}^{(b_x)}\left(x-d,\,0\right)+\frac{\mu(3-2\nu)}{2\pi(1-\nu)}\int_{-a}^{a}\frac{B_{II}(t)}{x-t}dt + \frac{\mu}{\pi}\int_{-a}^{a}B_{II}(t)R_4(x-t)dt \quad , \tag{78}$$

In view of the asymptotic relations (65) it is inferred that the shear stress σ_{yx} at the crack-tips exhibits a square-root singularity, as in the classical elasticity case.

Further, integrating Eq. (39) across the crack faces $\left(|x|<a,\,y=0\right)$ and employing results from asymptotic analysis, the couple-stress m_{xz} is evaluated as

$$m_{xz}\left(|x|>a,\,0\right)=m_{xz}^{(b_x)}\left(x-d,\,0\right)+\frac{\mu}{\pi}\int_{-a}^{a}B_{II}\left(t\right)\ln|x-t|dt+\frac{\mu}{\pi}\int_{-a}^{a}B_{II}\left(t\right)R_6\left(x-t\right)dt \quad , \tag{79}$$

where the regular kernel $R_6\left(x-t\right)$ is defined as

$$R_6\left(x-t\right)=\left[\frac{2\ell^2}{\left(x-t\right)^2}-K_2\left(\frac{|x-t|}{\ell}\right)\right]-\left[K_0\left(\frac{|x-t|}{\ell}\right)+\ln\left(\frac{|x-t|}{\ell}\right)\right]. \tag{80}$$

Regarding the asymptotic behavior of the couple-stress m_{xz} near the right crack tip, the following expressions hold for $x\to a^+$

$$\int_{-a}^{a}B_{II}\left(t\right)\ln|x-t|dt=O(1)\ ,\qquad \int_{-a}^{a}B_{II}\left(t\right)R_6\left(x-t\right)dt=O(1), \tag{81}$$

which imply that m_{xz} is bounded at the crack tip, verifying the asymptotic results obtained by Huang et al. (1997).

In Fig. 4a, the distribution of the shear stress σ_{yx} due to the interaction with a discrete glide dislocation lying at a distance $d/a=2.5$ is displayed in a couple-stress medium with $a/\ell=10$ and Poisson's ratio $\nu=0.3$. We observe that the Cosserat effects are visible within a zone of 7ℓ around the dislocation core and 2ℓ near the crack tip. Also, as $x\to d$, the shear stress retains the Cauchy type singularity reported in classical elasticity. On the other hand, the couple stress m_{xz} (Fig. 4b) exhibits a bounded negative value at the right crack tip and diminishes quickly to zero as $x>d$. On both sides of the discrete dislocation ($x=d$), the field changes from finite negative values to unbounded positive values, exhibiting a logarithmic singularity, as Eq. (39) suggests. It should be mentioned that for certain positions of the discrete defect, positive values of the couple-stress m_{xz} are reported in the range $0\le\bar{x}\le d-a$.

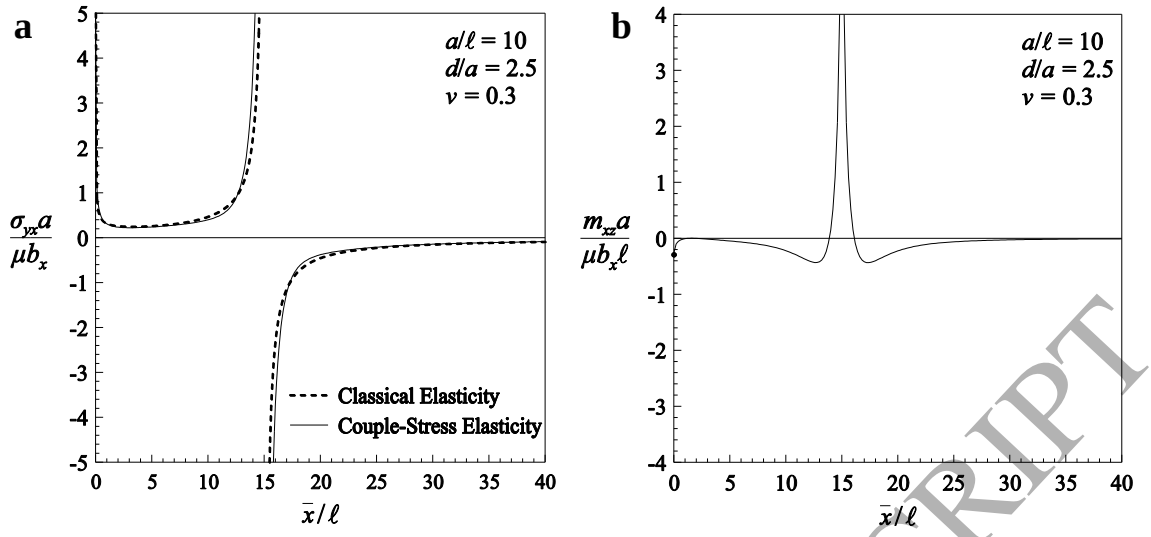

Fig. 4: Variation of **a)** the shear stress σ_{yx} and **b)** the couple-stress m_{xz} ahead of the right crack tip due to the interaction with a glide dislocation lying at $d/a = 2.5$ in a medium with $a/\ell = 10$ and Poisson's ratio $\nu = 0.3$.

The variation of the stress intensity factor (SIF) in both crack tips is examined next in the context of couple-stress theory. The SIF at the right crack tip (a similar definition can be given for the left crack tip) is defined as $K_{II} = \lim_{x \to a^+} \left[2\pi (x-a) \right]^{1/2} \sigma_{yx}(x, 0)$, where the shear stress $\sigma_{yx}(x, 0)$ is given by Eq. (78). In Fig. 5a, the deviation of the SIF in couple-stress theory from the classical elasticity prediction is highlighted by plotting the ratio $K_{II}/K_{II}^{clas.}$ in both crack tips with respect to the microstructural ratio ℓ/a and the Poisson's ratio ν for a glide dislocation placed at $d/a = 1.4$. It is observed that the SIF in couple-stress theory is higher when couple-stress effects are considered for any ℓ/a. As ℓ/a increases, all curves exhibit an initial decreasing response until a minimum value is reached in the range $0.1 \le \ell/a \le 0.15$ for the right crack tip (this range varies depending on the Poisson's ratio and the dislocation distance d/a). Then, the ratio increases monotonically tending to an asymptotic value of $(3-2\nu)$ as $\ell/a \to \infty$. For $\ell/a = 0$ a finite jump discontinuity is reported (i.e. $K_{II}/K_{II}^{clas.} \neq 1$), which is attributed to the severe boundary layer effects of couple-stress elasticity in singular stress-concentration problems (Sternberg and Muki, 1967; Gourgiotis and Georgiadis, 2007; 2008). It should be noted that the magnitude of this discontinuity,

equal to $(3-2\nu)^{1/2}$, is independent of the distance of the defect and significantly higher than the one observed in the interaction problem between a finite-length crack and a climb dislocation (see Part I, Fig. 8). Also, the same discontinuity has been observed in other problems where in-plane shear loading is applied to the crack faces (Gourgiotis and Georgiadis, 2007; Gourgiotis et al., 2012).

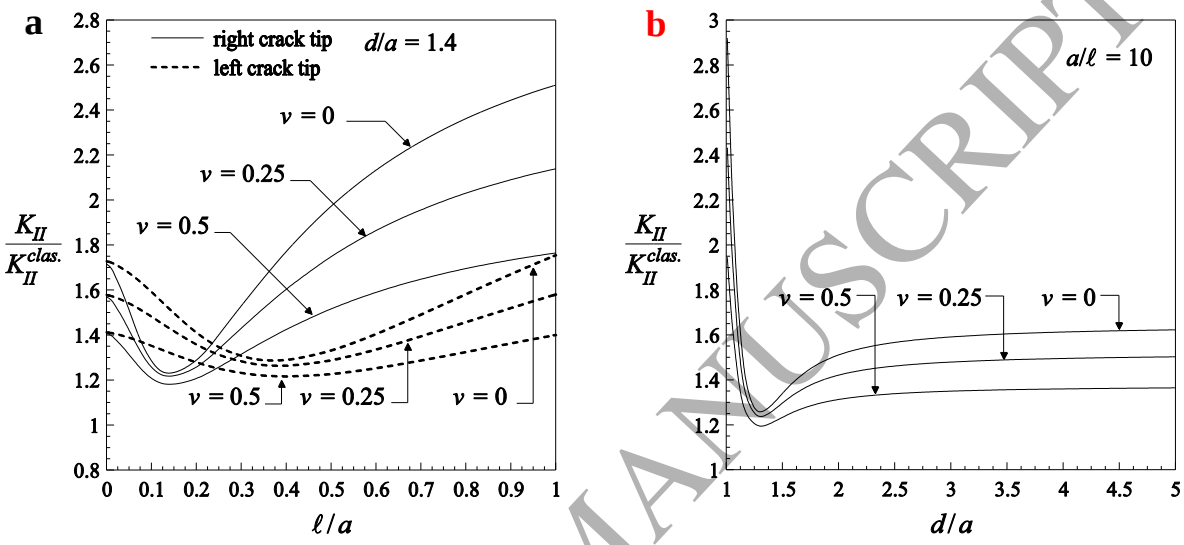

Fig. 5: **a)** Variation of the ratio of SIFs $K_{II}/K_{II}^{clas.}$ in couple-stress theory and in classical elasticity with ℓ/a for a glide dislocation lying at $d/a=1.4$. **b)** Variation of $K_{II}/K_{II}^{clas.}$ in the right crack-tip with the dislocation distance d/a in a material with $a/\ell=10$.

Moreover, in Fig. 5b, the variation of the ratio $K_{II}/K_{II}^{clas.}$ ahead of the right crack-tip is plotted for various values of the dislocation distance d/a and the Poisson's ratio ν in a medium with $a/\ell=10$. As d/a increases, all curves exhibit an initial decreasing response until a minimum value is reached in the range $1.25\le d/a\le 1.35$ for the right crack tip (this range varies depending on the Poisson's ratio and the ratio a/ℓ). Then, the ratio increases monotonically as the dislocation is placed farther from the crack-tip and quickly reaches a constant value. This value coincides with the corresponding value of the ratio in the problem of a finite-length crack under constant remote loading (mode II), for the same ratio a/ℓ. Indeed, Gourgiotis and Georgiadis (2007) reported a ratio of 1.66 for $\ell/a=0.1$ and $\nu=0$

while for $\nu = 0.25$ and $\nu = 0.5$ the values are 1.52 and 1.38, respectively. A similar response is observed at the left crack-tip.

Table 1: Convergence of the SIFs ratio $K_{II,r}/K_{II,r}^{clas.}$ at the right crack-tip for increasing collocation points N. The glide dislocation lies at a distance $d/a = 2.0$ in a couple-stress material with Poisson's ratio $\nu = 0$.

N	$\ell/a = 1.0$	$\ell/a = 0.8$	$\ell/a = 0.5$	$\ell/a = 0.2$	$\ell/a = 0.1$	$\ell/a = 0.05$	$\ell/a = 0.01$	$\ell/a = 0.005$
10	1.78048	1.55748	1.18799	1.24669	1.51183	1.66267	2.71730	2.96546
20	1.78051	1.55750	1.18801	1.24668	1.51058	1.63311	1.77377	2.12084
30	1.78051	1.55750	1.18801	1.24668	1.51058	1.63310	1.71490	1.75901
40						1.63310	1.71424	1.72635
50							1.71405	1.72338
60							1.71405	1.72335
70								1.72335

We proceed to the numerical evaluation of the energy release rate (*J*-integral) and the investigation of its dependence upon the characteristic length ℓ of couple-stress elasticity, the Poisson's ratio ν, and the distance d of the discrete defect from the crack tip. In Fig. 6, the variation of the ratio $J/J^{clas.}$ on both crack tips with respect to ℓ/a and the Poisson's ratio ν is presented for a glide dislocation lying at $d/a = 1.4$. The expressions for the *J*-integral in classical elasticity remain the same as in the interaction problem between a finite-length crack and a climb dislocation examined in Part I (see Eq. (48) in Part I). The plot reveals that as $\ell/a \to 0$, the ratio $J/J^{clas.}$ tends to unity, so that the *J*-integral in couple-stress theory converges to the corresponding result of classical elasticity. This behavior has been reported in other studies of crack problems in couple-stress theory (Atkinson and Leppington, 1977; Gourgiotis and Georgiadis, 2008; Gourgiotis et al., 2012). Similarly to the SIF response, the *J*-integral ratio does not exhibit a monotonic behaviour with respect to ℓ/a. Specifically, as ℓ/a increases, all curves exhibit an initial decreasing response $\left(J < J^{clas.}\right)$ until a minimum value is reached for $0.1 \le \ell/a \le 0.15$ (for the right crack tip) and then the ratio monotonically increases $\left(J > J^{clas.}\right)$. Therefore, depending on the ratio ℓ/a, the energy release rate in couple-stress theory may either decrease, compared to the classical value, revealing a strengthening effect, or increase predicting thus a weakening effect. The asymptotic value of the ratio $J/J^{clas.}$ as $\ell/a \to \infty$ is the same with the ratio of SIFs, that is $(3-2\nu)$.

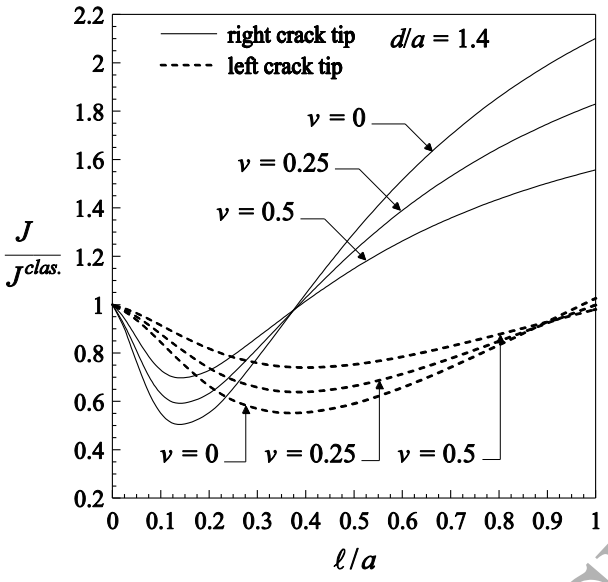

Fig. 6: Variation of the ratio of *J*-integrals in couple-stress theory and in classical elasticity with respect to the ratio ℓ/a for a glide dislocation lying at $d/a=1.4$.

A more detailed description of how the ratio of the energy release rates depends upon the material and geometrical characteristics of the cracked body is presented in Fig. 7. More specifically, Fig. 7 illustrates the level sets of $J/J^{clas.}$ (right crack tip) with respect to the ratios ℓ/a and d/a for a couple-stress material with Poisson's ratios $\nu=0$ (Fig. 7a) and $\nu=0.5$ (Fig. 7b). It is observed that below the contour $J/J^{clas.}=1$, the energy release rate, or equivalently the crack driving force, increases in couple-stress theory. This region, where the weakening effect ($J/J^{clas.}>1$) is predicted, reduces by a small percentage as the Poisson's ratio increases. However, comparing this response to the one obtained for the opening mode (Part I, Fig. 10), we conclude that the response varies significantly for the two plane problems. In the shear mode studied herein, the weakening effect is limited to smaller distances to the crack tip. Similar conclusions can be drawn by evaluating the driving Peach-Koehler force exerted on the discrete glide dislocation using its definition and the expression for the shear stress σ_{yx} (Eq. (78)).

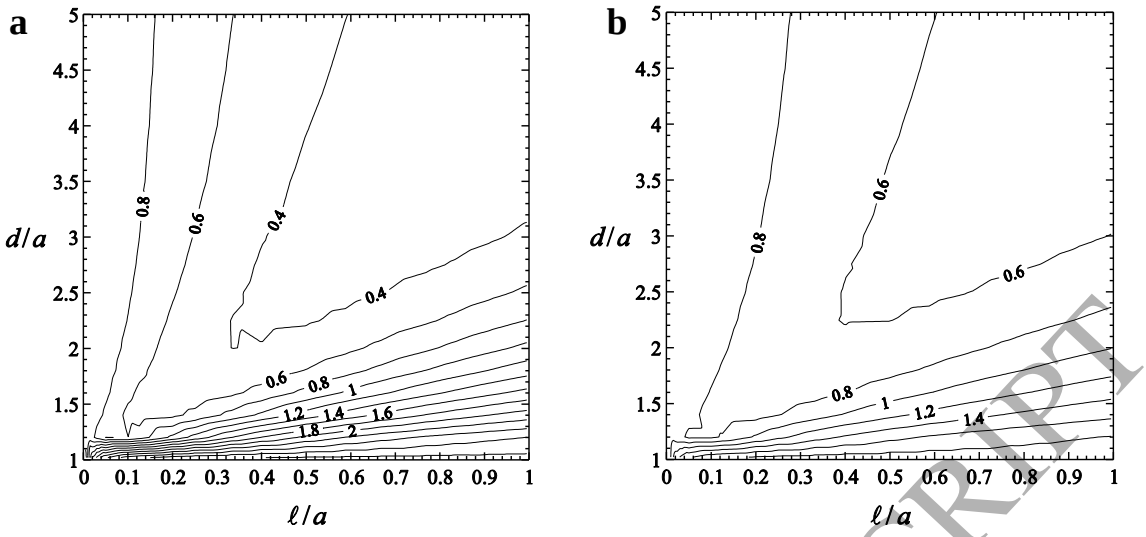

Fig. 7: Level sets of the ratio $J/J^{clas.}$ with respect to ℓ/a and d/a for Poisson's ratio **a)** $\nu=0$ and **b)** $\nu=0.5$.

7.2 Interaction of a finite-length crack with a screw dislocation

The discussion of the results for the antiplane crack problem is now in order. In Fig. 8, the dependence of the antiplane displacement w upon the ratio a/ℓ is plotted for a discrete screw dislocation lying at a distance $d/a=2.5$ in a couple-stress medium with $\beta=0$. Focusing on the detail of this figure, we observe that the crack faces near the crack tip close in a smoother way $\sim\bar{x}^{3/2}$ (as Eq. (72) suggests) compared to the classical elasticity prediction ($\sim\bar{x}^{1/2}$). This type of closure has been observed also in experimental studies where the crack tip remains sharp and not blunted up to the atomic scale (Elssner et al., 1994). Moreover, similarly to the plane problem presented earlier, it is noted that as the crack length becomes comparable to the characteristic length ℓ, the material exhibits a more stiff behaviour, that is, the crack-face displacements are smaller than those provided by classical elasticity. The latter solution serves as an upper bound for the couple-stress elasticity results.

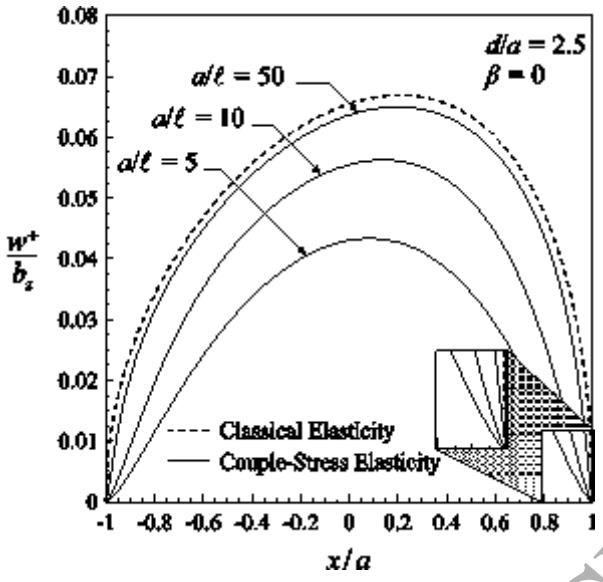

Fig. 8: Normalized upper-half crack antiplane displacement profile for various ratios a/ℓ due to the interaction with a screw dislocation lying at $d/a = 2.5$ in a material with $\beta = 0$.

The total shear stress t_{yz} ahead of the crack tip can be evaluated using Eq. (56)

$$t_{yz}\left(|x|>a,\,0\right)=t_{yz}^{(b_z)}\left(x-d,\,0\right)-c_1\ell^2\int_{-a}^{a}\frac{B_{III}\left(t\right)}{\left(x-t\right)^3}dt+c_2\int_{-a}^{a}\frac{B_{III}\left(t\right)}{x-t}dt+c_3\int_{-a}^{a}B_{III}\left(t\right)R_5\left(x-t\right)dt, \tag{82}$$

where the integrals in (82) are now regular. In addition, based on previous asymptotic considerations, the shear traction t_{yz} exhibits a higher-order singularity at the crack tip of the form $\bar{x}^{-3/2}$ as compared to the standard square-root singularity predicted by the classical theory. Such an asymptotic behavior has been reported also in the mode III problem in couple-stress theory (Gourgiotis and Georgiadis, 2007) and in dipolar gradient elasticity for both plane and antiplane strain modes (Georgiadis, 2003; Gourgiotis and Georgiadis, 2009).

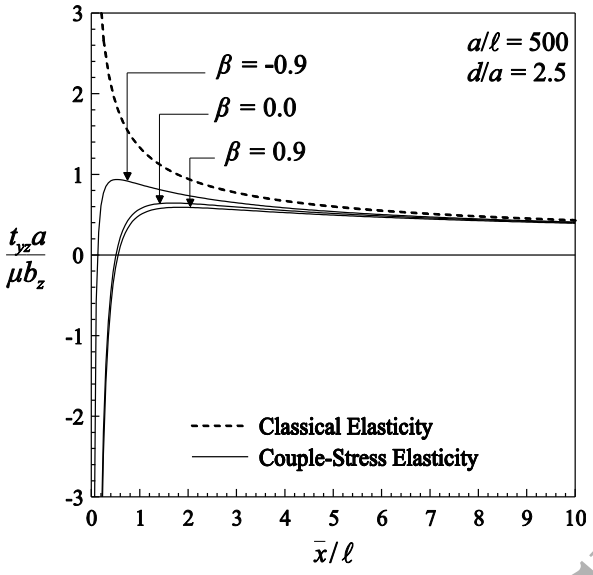

Fig. 9: Variation of the total shear stress t_{yz} ahead of the right crack tip due to the interaction with a screw dislocation lying at $d/a = 2.5$ in a medium with $a/\ell = 500$ for different values of β.

In Fig. 11, the distribution of the shear stress t_{yz} due to the interaction with a discrete screw dislocation lying at a distance $d/a = 2.5$ is presented, in a medium with $a/\ell = 500$ and three values of the parameter β. We observe that t_{yz} takes on negative values in a very small zone ahead of the right (and the left) crack tip $(\bar{x} < 0.5\ell)$, exhibiting, thus, a cohesive-traction character along the prospective fracture zone. Also, a bounded maximum value is noted for $\bar{x} < 2\ell$, which may be used a critical stress criterion for further advancement of the crack. For $\bar{x} > 2\ell$, the distribution of the total stress t_{yz} tends to the classical elasticity solution. Regarding the parameter β, it is noted that as $\beta \to -1$ the width of the cohesive-traction zone significantly reduces, while the maximum value of the total stress increases. A similar behavior has been reported in the mode III problem in couple-stress theory (Gourgiotis and Georgiadis, 2007) and in dipolar gradient elasticity (Georgiadis, 2003) and is also supported by experimental evidence (Prakash et al., 1992).

In Fig. 10, the variation of the ratio $J/J^{clas.}$ on both crack tips with respect to the ratio ℓ/a and the constant β is given, for a screw dislocation lying at $d/a = 2.5$. As in the plane strain cases, we note that as $\ell/a \to 0$ the energy release rate tends to the corresponding result of classical elasticity. However, contrary to the previous cases, the ratio $J/J^{clas.}$

exhibits a monotonically decreasing behavior as ℓ/a increases. This response is independent of the screw dislocation distance d/a. Consequently, the energy release rate reveals a strengthening effect in the antiplane problem when couple-stresses are considered. It is interesting to note that the ratio $J/J^{clas.}$ tends to zero for $\beta \geq 0$ and $\ell/a \geq 1$. This behavior has also been observed in strain gradient elasticity in the cases of mode I and mode II cracks (Gourgiotis and Georgiadis, 2009). Finally, it should be mentioned that, contrary to the plane strain problems, the ratio $J/J^{clas.}$ is always higher at the left crack tip.

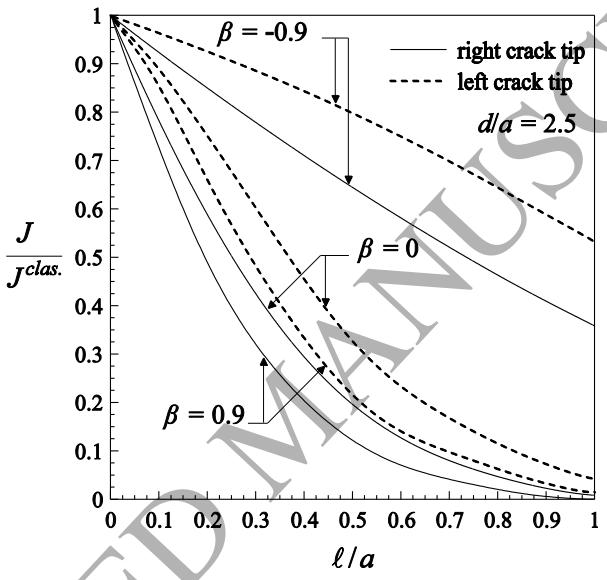

Fig. 10: Variation of the ratio of *J*-integrals in couple-stress theory and in classical elasticity with ℓ/a for a screw dislocation lying at $d/a = 2.5$.

Table 2: Convergence of the ratio $J_{,r}/J_{,r}^{clas.}$ at the right crack-tip for increasing collocation points N. The screw dislocation lies at a distance $d/a = 2.0$ in a couple-stress material with $\beta = -0.9$.

N	$\ell/a = 1.0$	$\ell/a = 0.8$	$\ell/a = 0.5$	$\ell/a = 0.2$	$\ell/a = 0.1$	$\ell/a = 0.05$	$\ell/a = 0.01$	$\ell/a = 0.005$
10	0.27016	0.37823	0.57837	0.81850	0.80671	0.17252	0.66546	2.55497
20	0.27017	0.37827	0.57839	0.81810	0.90653	0.95216	0.09993	0.22237
30	0.27017	0.37827	0.57839	0.81806	0.90681	0.95287	0.38653	0.09138
40				0.81806	0.90681	0.95287	0.95458	0.19633
50							0.99012	0.72165
60							0.99049	0.97271
70							0.99049	0.99431
80								0.99522
90								0.99522

8. Concluding remarks

In Part II of this investigation, the interaction problems between a finite-length crack and discrete glide and screw dislocations were examined in the framework of couple-stress elasticity. The distributed dislocation technique was employed to formulate the governing equations for both problems, which resulted, accordingly, in a singular and a hyper-singular integral equation for the plane and antiplane shear mode problems.

As in the opening mode problem examined in Part I of this study, a rigidity effect was observed in both shear mode cases. Moreover, it was shown that the couple-stress contribution is significant within a small zone adjacent to the crack tip and around the dislocation core. In the case of the glide dislocation loading, the evaluation of the energy release rate (J -integral) revealed an interesting 'alternating' behavior between strengthening and weakening of the crack as compared to the classical elasticity behavior. On the contrary, in the case of the screw dislocation loading the response is monotonic predicting always a strengthening effect when couple-stresses are considered.

As a final comment to this two-part investigation, it should be noted that, as a first approximation, the edge defects were assumed to lie along the crack plane. In the general case, a randomly oriented discrete edge dislocation may be considered at an angle off the crack plane. This configuration leads in a mixed mode problem where discrete climb, glide, and constrained wedge disclinations need to be distributed along the crack faces in order to produce a traction free crack. Further, for some orientations and locations of the dislocation, partial or full crack closure might occur and the problem has to be formulated following a different approach. It should be noted that this problem has not been extensively investigated even in classical elasticity (Comninou, 1987).

Acknowledgment

The authors are thankful to Prof. X. Markenscoff (University of California, San Diego) for fruitful discussions.

Appendix

In this Appendix, we provide the closed-form expressions for the singular and hyper-singular integrals involving Chebyshev polynomials that were utilized in Section 5. The singular integrals are calculated in the Cauchy principal value sense, while the hyper-singular integrals in the finite-part (F.P.) Hadamard sense. The following relations are reported for $|x|<1$ (see also Kaya and Erdogan, 1987; Chan et al., 2003)

$$\int_{-1}^{1}\frac{T_n(t)\left(1-t^2\right)^{-1/2}}{x-t}dt=\begin{cases}0\,, & n=0,\\ -\pi U_{n-1}(x)\,, & n\geq 1,\end{cases} \tag{A1}$$

$$\int_{-1}^{1}\frac{U_n(t)\left(1-t^2\right)^{1/2}}{x-t}dt=\pi T_{n+1}(x)\,,\quad n\geq 0\,, \tag{A2}$$

$$\begin{aligned}\text{F.P.}\int_{-1}^{1}\frac{U_n(t)\left(1-t^2\right)^{1/2}}{(x-t)^3}dt&=\\ &=\begin{cases}0, & n=0,\\ \dfrac{\pi}{4\left(1-x^2\right)}\left[\left(n^2+3n+2\right)U_{n-1}(x)-\left(n^2+n\right)U_{n+1}(x)\right], & n\geq 1,\end{cases}\end{aligned} \tag{A3}$$

where $T_n(t)$ and $U_n(t)$ are the Chebyshev polynomials of the first and second kind, respectively.

For $|x|>1$, the above integrals are no longer singular and are evaluated according to the following expressions

$$\int_{-1}^{1}\frac{T_n(t)\left(1-t^2\right)^{-1/2}}{x-t}dt=\pi\,\mathrm{sgn}(x)\frac{\left[x-\mathrm{sgn}(x)\left(x^2-1\right)^{1/2}\right]^n}{\left(x^2-1\right)^{1/2}}\,,\quad n\geq 0\,, \tag{A4}$$

$$\int_{-1}^{1}\frac{U_n(t)\left(1-t^2\right)^{1/2}}{x-t}dt=\pi\left[x-\mathrm{sgn}(x)\left(x^2-1\right)^{1/2}\right]^{n+1}\,,\quad n\geq 0\,, \tag{A5}$$

$$\int_{-1}^{1}\frac{U_n(t)\left(1-t^2\right)^{1/2}}{(x-t)^3}dt=\frac{\pi}{2}(n+1)\left[x-\operatorname{sgn}(x)\left(x^2-1\right)^{1/2}\right]^{n-1}$$
$$\times\left[n\left(1-\frac{|x|}{\left(x^2-1\right)^{1/2}}\right)^2+\frac{|x|-\left(x^2-1\right)^{1/2}}{\left(x^2-1\right)^{3/2}}\right],\quad n\geq 0\,. \tag{A6}$$

References

Atkinson, C., Leppington, F.G., 1977. The effect of couple stresses on the tip of a crack. Int. J. Solids Struct. 13, 1103-1122.

Bilby, B.A., Cottrell, A.H., Swinden, K.H., 1963. The spread of plastic yield from a notch. Proc. R. Soc. Lond. A 272, 304-314.

Bilby, B.A., Eshelby, J.D., 1968. Dislocations and the theory of fracture, in: Liebowitz, H. (Ed.), Fracture, Vol. 1. Academic Press, New York.

Chan, Y.-S., Fannjiang, A.C., Paulino, G.H., 2003. Integral equations with hypersingular kernels – theory and applications to fracture mechanics. Int. J. Eng. Sci. 41, 683-720.

Cohen, H., 1966. Dislocations in couple-stress elasticity. J. Math. Phys. 45, 35-44.

Comninou, M., 1987. The interaction between a dislocation and a crack: Closure considerations. Mech. Res. Commun. 14, 245-253.

Elssner, G., Korn, D., Ruehle, M., 1994. The influence of interface impurities on fracture energy of UHV diffusion bonded metal-ceramic bicrystals. Scripta Metall. Mater. 31, 1037-1042.

Georgiadis, H.G., 2003. The Mode III crack problem in microstructured solids governed by dipolar gradient elasticity: Static and dynamic analysis. J. Appl. Mech. 70, 517-530.

Gourgiotis, P., Georgiadis, H., Sifnaiou, M., 2012. Couple-stress effects for the problem of a crack under concentrated shear loading. Math. Mech. Solids 17, 433-459.

Gourgiotis, P.A., Georgiadis, H.G., 2007. Distributed dislocation approach for cracks in couple-stress elasticity: shear modes. Int. J. Fract. 147, 83-102.

Gourgiotis, P.A., Georgiadis, H.G., 2008. An approach based on distributed dislocations and disclinations for crack problems in couple-stress elasticity. Int. J. Solids Struct. 45, 5521-5539.

Gourgiotis, P.A., Georgiadis, H.G., 2009. Plane-strain crack problems in microstructured solids governed by dipolar gradient elasticity. J. Mech. Phys. Solids 57, 1898-1920.

Hills, D.A., Kelly, P.A., Dai, D.N., Korsunsky, A.M., 1996. Solution of crack problems: the distributed dislocation technique. Kluwer Academic Publishers.

Huang, Y., Zhang, L., Guo, T.F., Hwang, K.C., 1997. Mixed mode near-tip fields for cracks in materials with strain-gradient effects. J. Mech. Phys. Solids 45, 439-465.

Kaya, A.C., Erdogan, F., 1987. On the solution of integral equations with strongly strongly singular kernels. Q. Appl. Math. 45, 105-122.

Knésl, Z., Semela, F., 1972. The influence of couple-stresses on the elastic properties of an edge dislocation. Int. J. Eng. Sci. 10, 83-91.

Koiter, W., 1964. Couple stresses in the theory of elasticity. Parts I and II, Nederl. Akad. Wetensch. Proc. Ser. B, pp. 17-29.

Kutt, H.R., 1975. The numerical evaluation of principal value integrals by finite-part integration. Numer. Math. 24, 205-210.

Lubarda, V., 2003. Circular inclusions in anti-plane strain couple stress elasticity. Int. J. Solids Struct. 40, 3827-3851.

Mindlin, R.D., 1963. Influence of couple-stresses on stress concentrations. Exp. Mech. 3, 1-7.

Mindlin, R.D., Tiersten, H.F., 1962. Effects of couple-stresses in linear elasticity. Arch. Ration. Mech. Anal. 11, 415-448.

Mishuris, G., Piccolroaz, A., Radi, E., 2012. Steady-state propagation of a Mode III crack in couple stress elastic materials. Int. J. Eng. Sci. 61, 112-128.

Monegato, G., 1994. Numerical evaluation of hypersingular integrals. J. Comput. Appl. Math. 50, 9-31.

Muki, R., Sternberg, E., 1965. The influence of couple-stresses on singular stress concentrations in elastic solids. ZAMP 16, 611-618.

Nowacki, W., 1974. On discrete dislocations in micropolar elasticity. Arch. Mech. 26, 3-11.

Prakash, V., Freund, L.B., Clifton, R.J., 1992. Stress wave radiation from a crack tip during dynamic initiation. J. Appl. Mech. 59, 356-365.

Radi, E., 2008. On the effects of characteristic lengths in bending and torsion on Mode III crack in couple stress elasticity. Int. J. Solids Struct. 45, 3033-3058.

Sternberg, E., Muki, R., 1967. The effect of couple-stresses on the stress concentration around a crack. Int. J. Solids Struct. 3, 69-95.

Toupin, R.A., 1962. Perfectly elastic materials with couple stresses. Archive of Rational Mechanics and Analysis 11, 385–414.

Zhang, L., Huang, Y., Chen, J.Y., Hwang, K.C., 1998. The mode III full-field solution in elastic materials with strain gradient effects. Int. J. Fract. 92, 325-348.

Zhang, T.-Y., Li, J.C.M., 1991. Image forces and shielding effects of a screw dislocation near a finite-length crack. Mat. Sci. Eng. A 142, 35-39.